Observations of the collapse of asymmetrically driven convergent shocks

J. R. Rygg,[1,a)] J. A. Frenje,[1] C. K. Li,[1] F. H. Séguin,[1] R. D. Petrasso,[1,b)] F. J. Marshall,[2] J. A. Delettrez,[2] J. P. Knauer,[2] D. D. Meyerhofer,[2,c)] and C. Stoeckl[2]
[1]*Plasma Science and Fusion Center, Massachusetts Institute of Technology, Cambridge, Massachusetts 02139, USA*
[2]*Laboratory for Laser Energetics, University of Rochester, Rochester, New York 14623, USA*

(Received 23 October 2007; accepted 15 February 2008; published online 26 March 2008)

The collapse of strong convergent shocks in spherical geometry is observed using measurements of induced nuclear production and x-ray emission. Precise and absolute measurements of the timing and yield of nuclear production induced by the collapse of laser-driven shocks give the same results when shocks are launched by uniform (<2% rms) or nonuniform (up to 32% rms) laser illumination. The observation was repeated for both low-mode (dominated by spherical harmonic modes $\ell=1-2$) and high-mode ($\ell=31-500$) drive asymmetries. For low-mode nonuniform drive, the center of collapse as observed through x-ray emission shifts away from target center toward the direction of low intensity. The x-ray emission brightness is seen to drop precipitously with larger low-mode drive asymmetry, in stark contrast to the drive-uniformity insensitivity of nuclear yields at the time of shock collapse. © *2008 American Institute of Physics*. [DOI: 10.1063/1.2892025]

The propagation of strong convergent shocks in spherical geometry has been investigated in the context of diverse fields of physics, including core-collapse supernovae,[1] sonoluminescence,[2] and inertial confinement fusion (ICF).[3,4] Analytic and computational studies have indicated that initial deviations of a shock front from sphericity are expected to grow geometrically as the shock converges,[5,6] which could be of concern in situations where a high degree of symmetry is necessary, such as in ICF implosions.

Observations of shock-induced nuclear production in capsule implosions reported elsewhere[7–9] have used symmetric initial conditions, although asymmetries have been observed in the degree of shell compression at the time of shock collapse.[7,8] The effects of imposed drive nonuniformities on capsule implosions have been studied in the context of correlated compression asymmetries near stagnation time,[10] as well as the growth of compression asymmetries from shock collapse time to stagnation time.[11,8] This brief communication reports detailed and systematic experimental studies of the effects of asymmetric convergence on shock collapse, using imaging and temporal measurements of x-ray and nuclear product emission induced by the collapse of strong symmetrically and asymmetrically driven convergent spherical shocks.

The imploding shocks were driven in spherical targets by intense (10^{15} W/cm^2) laser illumination using the OMEGA laser system.[12] OMEGA's 60 laser beams delivered 22 to 24 kJ total laser energy uniformly to the targets, using a 0.351 μm wavelength, 1 ns flat-top laser pulse. Except where otherwise noted, the uniformity of individual beams was enhanced using distributed phase plates, polarization smoothing, and two-dimensional smoothing by spectral dispersion with a 1 THz bandwidth.[13] These factors lead to a total on-target illumination nonuniformity of <2% rms for the nominally symmetric configuration.[14]

The targets were spherical plastic (CH) capsules with diameters of 860 and 930 μm, and shell thicknesses of 20, 24, 26, and 27 μm. The capsules were filled with an equimolar (by atom) mixture of deuterium (D_2) and helium-3 (^{3}He) gas to an initial mass density of 2.5 mg/cm^3.

To investigate the effects of low-mode drive nonuniformities on shock timing and nuclear production, three campaigns of targets with shell thicknesses of 24, 26, and 27 μm were conducted where the capsules were offset from the laser beam pointing center (BPC) by 0, 50, 100, and 150 μm, while the laser beams remained pointed at the nominal, no-offset target position. The resulting intensity nonuniformity is dominated by low spherical harmonic ℓ modes ($l=13$), with peak-to-valley intensity ratios of 1.4, 2.1, and 2.9 and surface-averaged root-mean-square (rms) variations of 11%, 21%, and 32% for offsets of 50, 100, and 150 μm, respectively.[15] The illumination intensity profiles and a schematic of the target offset are shown in Fig. 1.

To investigate the effects of high-mode drive nonuniformities on shock timing and convergence, capsules with 20 μm thick shells were driven without enhanced beam smoothing, which increases illumination nonuniformity in high spherical harmonic ℓ modes ($\ell=31\,500$) by a factor of 20.[13] The resulting overall laser intensity nonuniformity is increased to 14% rms without enhanced smoothing, compared to <2% rms with full beam smoothing.

The collapse and subsequent rebound of the strong converging shock heats the fill gas sufficiently (to 6 keV)[9] for the D^{3}He nuclear reaction, D+^{3}He$\rightarrow^4$He+p, to proceed. The temporal emission history of 14.7 MeV D^{3}He protons was measured using the proton temporal diagnostic (PTD) (Fig. 2),[8] which has a shot-to-shot timing accuracy of 25 ps. Absolute D^{3}He proton spectral measurements[16] are used in combination with the PTD signal to infer the D^{3}He reaction rate history.[8]

[a)]Now at Lawrence Livermore National Laboratory.
[b)]Also Visiting Senior Scientist at LLE.
[c)]Also Departments of Mechanical Engineering and Physics and Astronomy.

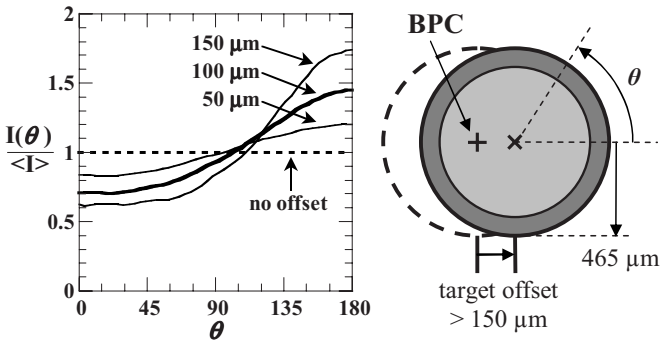

FIG. 1. Initial intensity profile (normalized to the surface average) on the surface of a capsule which has been displaced from laser beam pointing center (BPC). The angle θ is measured with respect to the direction of offset. The ~900 μm diameter capsules were displaced by up to 150 μm from BPC.

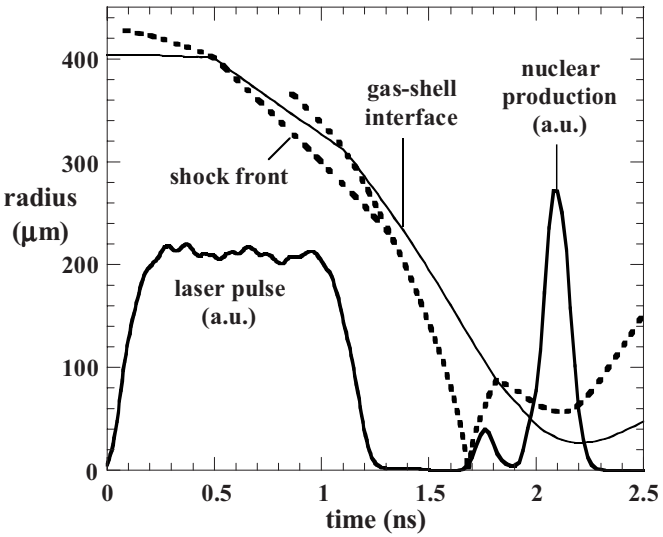

FIG. 3. One-dimensional numerical hydrodynamic simulation of a spherically symmetric implosion (OMEGA shot 38525) shows that D^3He nuclear production starts shortly after the collapse of the converging shock.

Two distinct periods of D^3He-proton emission are typically observed in CH capsule implosions (Fig. 2): the "shock-burn" is induced by heating of the gas by collapse and reflection of the convergent shock at the capsule center; the "compression burn" occurs as the fill gas is compressed and reheated by the imploding capsule shell. One-dimensional hydrodynamic simulations of symmetrically driven capsules using the code LILAC[17] show that the first nuclear reaction peak (observed at about 1.7 ns in Fig. 2) is emitted immediately after the collapse of the ingoing shock (see Fig. 3). The second, "compression" peak occurs about 300 ps later, and is induced by the nearly adiabatic compression and heating of the fill gas by the imploding shell.

When the converging shock is driven by an asymmetric laser drive, the launched shock has a local initial speed u_s that scales as the square root of the local ablation pressure (P_a). This pressure is generated by ablation of capsule material when absorbing energy deposited by the laser. P_a in turn

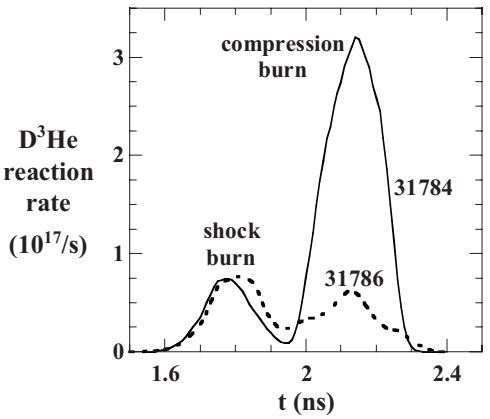

FIG. 2. The measured D^3He reaction rate from implosions of 26 μm thick plastic shells filled with D^3He gas shows two distinct periods of nuclear production. Shock burn is induced by shock collapse at about 1.65 ns and ends as the reflected shock encounters the imploding shell. The compression burn, after 2.0 ns, occurs as the imploding shell compresses and reheats the fill gas. Compression burn is substantially diminished when the target is offset 100 μm from BPC (shot 31786) compared to that from a centered target (shot 31784); however, the shock burn is not significantly affected by this large drive asymmetry.

scales as the 2/3 power of the local illumination intensity I,[3] so the shock speed scales as $u_s \sim [(I(\theta,\varphi)]^{1/3}$. Thus, for example, for targets displaced by 100 μm, the initial shock speed on the high-intensity side will be 27% faster than on the low intensity side (due to the 2.06 peak-to-valley intensity ratio).

According to the analytic and numerical analysis of Gardner *et al.*,[5] deviations from sphericity of the position of the shock front as a fraction of the mean shock radius ($\delta r/r$) increase as the shock converges, and also oscillate for modes $\ell > 1$. Considering a monatomic ideal gas in the small amplitude limit ($\delta r/r < 1\%$), the $\ell = 1$ asymmetry mode grows as $r^{-0.451}$, corresponding to a drift of the center. Asymmetry modes with $\ell > 1$ oscillate with a frequency that increases with ℓ, and amplitude given by $r^{-0.725}$.

One would expect that a collapsing shock with $\delta r/r \approx 1$ would be observably distinct from one with $\delta r/r \ll 1$. Although the initial shock asymmetries launched in these experiments is well above the small amplitude limit (~5% per 100 μm initial offset when the shock breaks into the gas), propagating the asymmetries inwards using this method indicates that $\delta r/r$ approaches 100% when the shock has converged by a factor of between 10 and 100.

The experimentally observed time of peak shock-induced nuclear production (shock-bang time) is minimally affected by illumination nonuniformities generated by displacing the target from BPC. Figure 4(a) shows the difference between shock-bang time of each offset target implosion with the corresponding centered target implosion shot with the same configuration on the same day.

The observed shock-induced D^3He nuclear yield is also not significantly affected by increased radiation nonuniformity produced by displacement of the target from BPC. The yield from each implosion in an offset campaign was normalized to the yield from the centered reference shot from the same campaign, and is shown in Fig. 4(b). The yield is not significantly degraded for offsets up to 100 μm, while an

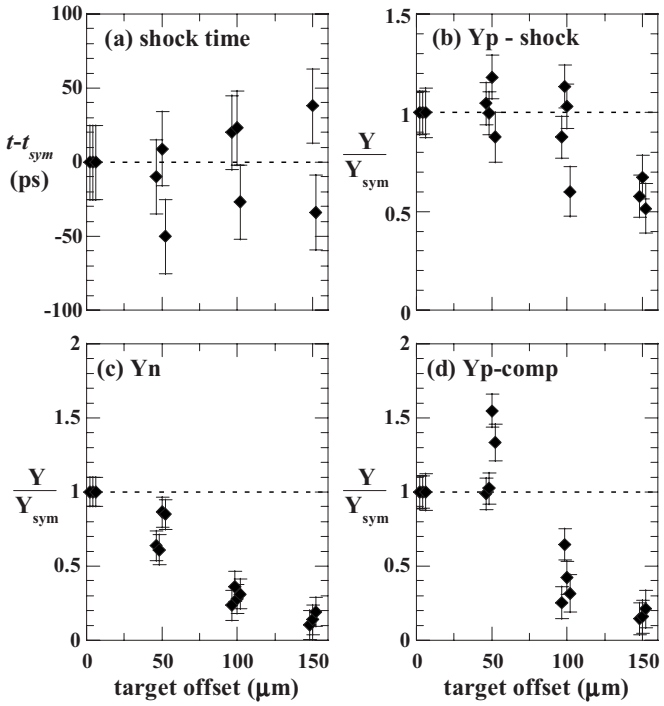

FIG. 4. Measured (a) shock-bang time, (b) D^3He shock yield, (c) DD-n compression yield (Ref. 18), and (d) D^3He compression yield for implosions of capsules displaced from beam pointing center (BPC) by up to 150 μm. Values of offset target shots are adjusted using values from the equivalent centered target shot with symmetric illumination. The difference in shock-bang times is less than the shot to shot scatter for all offsets. No significant reduction in D^3He shock yield is observed until the target is offset by 150 μm.

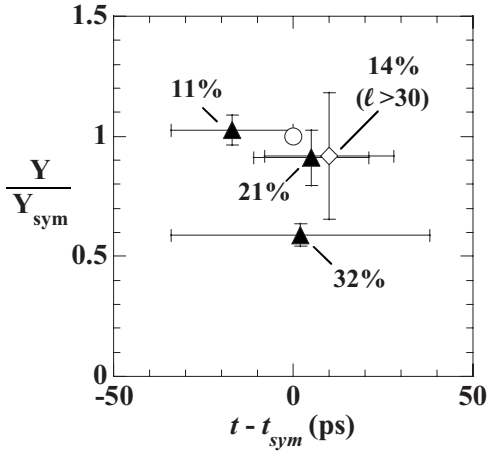

FIG. 5. Asymmetrically driven shocks have the same D^3He shock yield and shock-bang time performance as symmetric shocks driven through equivalent capsules. The shock yield ratio is plotted as a function of the shock-bang time delay as compared to the corresponding symmetric shot [open circle at (0,1)]. Shocks driven with low-mode ($\ell=1-3$, solid triangles) asymmetries less than 22% rms produce the same yield and timing, whereas a 32% rms degrades the yield by a factor of 2, without affecting timing. Shocks driven with high-mode ($\ell=31-500$, open diamond) asymmetries of 14% rms behave the same as the corresponding symmetrically driven shot.

offset of 150 μm results in a shock yield reduction of only 40%. In comparison, the DD-n (Ref. 18) and D^3He compression yields are reduced by factors of 8 and 10, respectively, for the 150 μm offset implosions. Capsule shell thickness had no observable effect on the trends of yields and timing with capsule offset (Fig. 4 plots data from all campaigns).

The observed yield and timing of shock-induced nuclear production also have minimal sensitivity to high ℓ-mode irradiation nonuniformities. Observations of capsule implosions without enhanced beam uniformity show shock yield reduced by $8\pm26\%$, and shock-bang time delayed by 10 ± 18 ps, compared to equivalent implosions with enhanced beam smoothing.

The overall robustness of the D^3He shock yield and shock-bang time to asymmetrically driven shocks is revealed in Fig. 5. The mean normalized shock yield is plotted against the mean shock time difference for each asymmetric configuration (50, 100, and 150 μm offsets; no enhanced beam smoothing). The errors represent the standard deviation of the mean for each configuration.

In contrast to the results from D^3He emission at shock time, observations of x-ray emission from the fill gas shortly after shock collapse show distinctly different behavior for symmetric and asymmetric drive illumination. X-ray emission was measured using a gated microscope x-ray imaging system.[19] Figure 6 shows x-ray images taken in a nominally symmetric implosion (a), and in implosions driven in capsules displaced by up to 150 μm from BPC (b–d). The 4–7 keV x-ray images comprised an 80 ps integration centered 0.1 ± 0.1 ns after the time of peak D^3He-proton shock emission.[20] The intensity of x-ray emission induced by the shock diminishes with larger offsets, until at 150 μm, no shock emission was observed. For offsets of 50 and 100 μm, collapse of the asymmetric shock is displaced from the center of the target by about half the displacement of the target from BPC.[21]

The extremely low sensitivity of the D^3He shock yield to grossly asymmetric converging shocks is especially unexpected in light of the dramatic differences seen in the x-ray images (Fig. 6), particularly the lower brightness of the x-ray emission region for larger offsets. If the shock energy for displaced targets collapses into a larger plasma volume than for centered targets, then the plasma temperature should be correspondingly lower, resulting in lower x-ray emissivity. However, the D^3He reactivity is extremely sensitive to temperature ($\sim T_i^6$ at 6 keV)[22] compared to the x-ray emissivity ($\sim T_e^{1/2}$ for photon energy equal to the electron temperature[23]), so lower x-ray brightness would correspond to dramatically reduced D^3He yield, if due to temperature alone.

X-ray and D^3He-proton emission not only have different temperature sensitivities, but also depend on temperatures of different particle species (electron T_e and ion T_i, respectively), which are raised through different mechanisms. The shock primarily heats the ions, which collisionally heat the electrons. The electron-ion thermal equilibration time (τ_{ei}) is comparable to the duration of the shock burn for the relatively low density and high temperature of the shocked plasma. One would expect that if the x-ray brightness is reduced due to a less "coherent" shock collapse, that the D^3He shock yield, with its high temperature sensitivity, would be

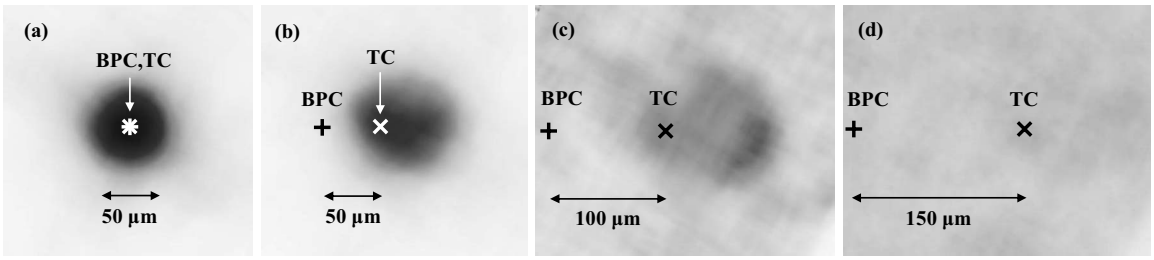

FIG. 6. 4–7 keV x-ray self-emission images from the fill gas near target center (TC, ×), 0.1 ± 0.1 ns after shock-bang time. The 930 μm diameter capsules of OMEGA shots (a) 31784, (b) 31790, (c) 31786, and (d) 31789 were displaced from the beam pointing center (BPC, +) by 0, 52, 107, and 154 μm, respectively. Whereas the shock collapses at TC for the centered target (a), for displaced targets (b, c), the shock collapses on the opposite side of TC from BPC, by about half the distance. For a TC offset of 154 μm (d), x-ray emission due to the collapsed shock was not observed.

even more severely extinguished, so it is not obvious how to reconcile this apparent discrepancy on the basis of thermal equilibration.

In summary, the first detailed and systematic experimental studies of the effects of asymmetric convergence on shock collapse were performed, where convergent shocks were launched in spherical capsules with both symmetric and asymmetric laser drives, and the shock collapse was observed using imaging and temporal measurements of x rays and D^3He nuclear products. The timing of shock collapse and the D^3He shock yield were observed to be insensitive to both low-mode and high-mode ($\ell = 31-500$) drive asymmetries. In contrast, x-ray emission brightness and D^3He compression yield were reduced dramatically with increased low-mode ($\ell = 1$) drive asymmetry, as the center of collapse shifts toward the side of low drive intensity.

The authors express their gratitude to the OMEGA engineers and operations crew who supported these experiments.

This work was supported in part by the U.S. Department of Energy Office of Inertial Confinement Fusion (Grant No. DE-FG03-03NA00058), by the Fusion Science Center for Extreme States of Matter and Fast Ignition (Contract No. 412761-G), by the Laboratory for Laser Energetics (Subcontract No. 412160-001G) under Cooperative Agreement DE-FC52-92SF19460, University of Rochester, and New York State Energy Research and Development Authority, and by the Lawrence Livermore National Laboratory (Subcontract No. B543881).

[1] H. A. Bethe, Rev. Mod. Phys. **62**, 801 (1990).
[2] M. P. Brenner, S. Hilgenfeldt, and D. Lohse, Rev. Mod. Phys. **74**, 425 (2002).
[3] J. Lindl, Phys. Plasmas **2**, 3933 (1995).
[4] S. Atzeni and J. Meyer-Ter-Vehn, *The Physics of Inertial Fusion* (Oxford University Press, New York, 2004).
[5] J. H. Gardner, D. L. Book, and I. B. Bernstein, J. Fluid Mech. **114**, 41 (1982).
[6] A. K. Evans, Phys. Rev. E **54**, 5004 (1996).
[7] R. D. Petrasso, J. A. Frenje, C. K. Li *et al.*, Phys. Rev. Lett. **90**, 095002 (2003).
[8] J. A. Frenje, C. K. Li, F. H. Séguin *et al.*, Phys. Plasmas **11**, 2798 (2004).
[9] J. R. Rygg, J. A. Frenje, C. K. Li *et al.*, "Dual nuclear product observations of shock collapse in inertial confinement fusion," Phys. Rev. Lett. (submitted).
[10] C. K. Li, F. H. Séguin, J. A. Frenje *et al.*, Phys. Rev. Lett. **92**, 205001 (2004).
[11] F. H. Séguin, R. D. Petrasso, J. A. Frenje *et al.*, Bull. Am. Phys. Soc. **47**, 144 (2002); F. H. Séguin, J. R. Rygg, J. A. Frenje *et al.*, *ibid.* **48**, 57 (2003).
[12] T. R. Boehly, D. L. Brown, R. S. Craxton *et al.*, Opt. Commun. **133**, 495 (1997).
[13] S. Skupsky and R. S. Craxton, Phys. Plasmas **6**, 2157 (1999).
[14] F. J. Marshall, J. A. Delettrez, R. Epstein *et al.*, Phys. Plasmas **11**, 251 (2004).
[15] The asymmetric drive described here is not enough to significantly accelerate the capsule center of mass (COM). For example, at the end of the laser pulse for the extreme 150 μm offset case, the kinetic energy associated with translational motion of the COM is only 2% of the total kinetic energy of the imploding shell.
[16] F. H. Séguin, J. A. Frenje, C. K. Li *et al.*, Rev. Sci. Instrum. **74**, 975 (2003).
[17] J. A. Delettrez, R. Epstein, M. C. Richardson *et al.*, Phys. Rev. A **36**, 3926 (1987).
[18] The measured total DD-n yield is dominated by emission during compression burn. Although not measured during this campaign, under similar conditions the shock-burn typically contributes only ~1% to the total DD-n yield (Ref. 9).
[19] F. J. Marshall and J. A. Oertel, Rev. Sci. Instrum. **68**, 735 (1997).
[20] Significant uncertainty in x-ray image timing allows a ~0.2 ns range of possible sample times for each shot. However, no evidence is seen in the images of x-ray emission from the imploding shell, as occurs during the compression-burn phase of the implosion ($t > 2.0$ ns).
[21] A simple analysis that neglects shock strengthening due to convergence gives a shock collapse displacement 0.75 times the target offset distance (compared to the ~0.5 observed).
[22] H.-S. Bosch and G. M. Hale, Nucl. Fusion **32**, 611 (1992).
[23] Ya. B. Zel'dovich and Yu. Raizer, *Physics of Shock Waves and High-Temperature Hydrodynamic Phenomena* (Dover, New York, 2002).